

DOI: 10.1002/cbic.201100587

# Inactivation of Glucosamine-6-Phosphate Synthase by $N^3$ -Oxoacyl Derivatives of L-2,3-Diaminopropanoic Acid

 Robert Jędrzejczak,<sup>[a]</sup> Marek Wojciechowski,<sup>[b]</sup> Ryszard Andruszkiewicz,<sup>[b]</sup> Paweł Sowiński,<sup>[c]</sup> Agata Kot-Wasik,<sup>[d]</sup> and Sławomir Milewski<sup>\*,[b]</sup>

$N^3$ -Oxoacyl derivatives of L-2,3-diaminopropanoic acid **1–4**, containing either an epoxide group or a conjugated double bond system, inactivate *Saccharomyces cerevisiae* glucosamine-6-phosphate (GlcN-6-P) synthase in a time- and concentration dependent manner. The results of kinetics studies on inactivation suggested a biphasic course, with formation of the enzyme–ligand complex preceding irreversible modification of the enzyme. The examined compounds differed markedly in their affinity to the enzyme active site. Inhibitors containing a phenyl ketone moiety bound much more strongly than their methyl ketone counterparts. The molecular mechanism of enzyme inactivation by phenyl ketone compounds **1** and **3**

was elucidated by using a stepwise approach with 2D NMR, MS and UV–visible spectroscopy. A substituted thiazine derivative was identified as the final product of a model reaction between an epoxide compound, **1**, and L-cysteine ethyl ester (CEE); and the respective cyclic product, found as a result of reaction between **1** and CGIF tetrapeptide, was identical to the N-terminal fragment of GlcN-6-P synthase. On the other hand, the reaction of a double-bond-containing compound, **3**, with CEE, CGIF and GlcN-6-P synthase led to the formation of a C–S bond, without any further conversion or rearrangement. Molecular mechanisms of the reactions studied are proposed.

## Introduction

L-Glutamine is a substrate for several enzymes known as amidotransferases; these catalyse the transfer of a  $\gamma$ -amide nitrogen from L-Gln to various acceptor molecules.<sup>[1]</sup> One of the amidotransferases, glucosamine-6-phosphate synthase (GlcN-6-P synthase), which uses D-fructose-6-phosphate (Fru-6-P) as an acceptor substrate, is the subject of interest as a potential target for antifungal chemotherapy and for possible pharmacological intervention in insulin-independent diabetes mellitus.<sup>[2,3]</sup> Thus the molecular properties of the enzyme have been extensively studied, including determination of the crystal structure of its bacterial version (as an intact protein and in complexes with several substrates, substrate analogues, products and inhibitors).<sup>[4]</sup> The results of these studies showed that *E. coli* GlcN-6-P synthase is a dimer of two identical subunits, each composed of two functional domains: the glutamine amide-hydrolysing domain (GAH) and the sugar phosphate-isomerising domain (ISOM), connected by an intramolecular channel. The catalytic mechanism is complex and involves: 1) Fru-6-P binding at ISOM, which triggers GAH ordering and assembly of the interdomain channel; 2) L-Gln binding at GAH, hydrolysis of its amide and ammonia transfer to ISOM through the channel; and 3) formation of the fructoseimine intermediate and its subsequent isomerisation to the final product, GlcN-6-P.<sup>[5]</sup> Much less structural data is available for eukaryotic versions of GlcN-6-P synthase, as so far only the crystal structures of the ISOM domains of *Candida albicans* and human enzymes have been determined,<sup>[6,7]</sup> but there is little doubt that the mechanism of catalysis in eukaryotic and prokaryotic GlcN-6-P synthases is exactly the same.

It is believed that inhibitors of GlcN-6-P synthase have the potential to become new drugs. Several such compounds (substrate analogues, transition-state-analogue inhibitors and heterocyclic compounds that inhibit enzyme dimerisation) have been described.<sup>[4,8]</sup> These include a number of glutamine analogues,  $N^3$ -acyl derivatives of L-2,3-diaminopropanoic acid that inhibit/inactivate GlcN-6-P synthase.  $N^3$ -(4-methoxyfumaroyl)-L-2,3-diaminopropanoic acid (FMDP) is one of the strongest inhibitors of GlcN-6-P synthase known to date. It inactivates the enzyme in a time- and concentration-dependent manner by forming a covalent bond with the catalytic Cys1 residue at the enzyme active site.<sup>[9]</sup> The molecular mechanism of GlcN-6-P inactivation by FMDP, established by Badet and co-workers, involves a Michael-type addition of Cys1 to the fumaroyl double-

[a] Dr. R. Jędrzejczak  
Present address: Midwest Center for Structural Genomics and Structural Biology Center, Biosciences, Argonne National Laboratory Building 202, 9700 South Cass Avenue, Argonne, IL 60439 (USA)

[b] Dr. M. Wojciechowski, Dr. R. Andruszkiewicz, Dr. S. Milewski  
Department of Pharmaceutical Technology and Biochemistry  
Gdańsk University of Technology  
11/12 Narutowicza Str., 80-233 Gdańsk (Poland)  
E-mail: slamilew@pg.gda.pl

[c] Dr. P. Sowiński  
Intercollegiate NMR Laboratory, Gdańsk University of Technology  
11/12 Narutowicza Str., 80-233 Gdańsk (Poland)

[d] Dr. A. Kot-Wasik  
Department of Analytical Chemistry, Gdańsk University of Technology  
11/12 Narutowicza Str., 80-233 Gdańsk (Poland)

Supporting information for this article is available on the WWW under <http://dx.doi.org/10.1002/cbic.201100587>.

bond, followed by two consecutive rearrangements, thus leading finally to the formation of a substituted 1,4-thiazin-3-one ring.<sup>[10]</sup>

During the course of our search for novel inhibitors of fungal GlcN-6-P synthases, several derivatives of *N*<sup>3</sup>-oxoacyl-L-2,3-diaminopropanoic acid were synthesised and found to be effective inhibitors of the target enzyme.<sup>[11]</sup> Now, evidence for the molecular mechanism of GlcN-6-P synthase inactivation by these compounds is presented. The biological model used in this study was the *Saccharomyces cerevisiae* enzyme, overproduced in host cells, purified to near homogeneity and characterised for its basic molecular and catalytic properties.

## Results

### Isolation and characterisation of yeast GlcN-6-P synthase

When grown in YPD medium, the YRS23-3 transformant, which contains the original *GFA1* gene under the control of a *PGK1* promoter, reproducibly expressed *S. cerevisiae* GlcN-6-P synthase at 5–7% of total cytoplasmic protein, as revealed by densitometric SDS-PAGE analysis. The enzyme was purified to at least 98% homogeneity with 42% final yield, by using the six-step procedure described in the Experimental Section. The  $K_m$  of the pure enzyme was 0.74 mM for L-Gln, 0.39 mM for D-Fru-6-P, and  $k_{cat}$  was 35.5 s<sup>-1</sup>. Pure GlcN-6-P synthase was chromatofocused on a MonoP HR 5/5 fast protein liquid chromatography (FPLC) column with a pH 6 to 4 gradient. The enzyme was partially denatured during column development, but the activity profile (not shown) enabled estimation of an isoelectric point of 5.35 ± 0.05. This value is lower than the 6.01 calculated for the known amino acid composition of the protein, but a similar phenomenon was previously found for the *Escherichia coli* and *C. albicans* counterparts of the yeast GlcN-6-P synthase.<sup>[12,13]</sup> The molecular weight ( $M_w$ ) of the native protein was determined by size exclusion chromatography at 320 ± 2 kDa, while the  $M_w$  of the Gfa1p subunit determined by SDS-PAGE was 80 ± 0.5 kDa. The latter value is in agreement with the theoretical  $M_w$  (79.916 kDa) calculated from the known amino acid sequence. It is most likely that native yeast GlcN-6-P synthase is a homotetramer (i.e. of identical subunits), as was previously shown for some other eukaryotic versions of this enzyme.<sup>[4]</sup> The pure enzyme was inhibited by uridine diphosphate *N*-acetylglucosamine (UDP-GlcNAc) with IC<sub>50</sub> = 0.52 mM. The inhibition was non-competitive with respect to L-Gln and uncompetitive with respect to D-Fru-6-P, thus suggesting that the UDP-GlcNAc binding site is not the enzyme active centre and indicating preferential binding of the inhibitor to the enzyme:Fru-6-P complex. It is highly probable that the UDP-GlcNAc-binding site is located in the *S. cerevisiae* enzyme in a similar manner as was shown for the truncated version of *C. albicans* Gfa1p.<sup>[6]</sup> Amino acid residues constituting the centre in *C. albicans* Gfa1p are completely conserved in the yeast enzyme, as shown in Figure 1. Yeast GlcN-6-P synthase was chosen as a biological model for the studies on enzyme inactivation because of its appropriate N-terminal amino sequence: a chymotrypsin cleavage site is present close to the N termi-

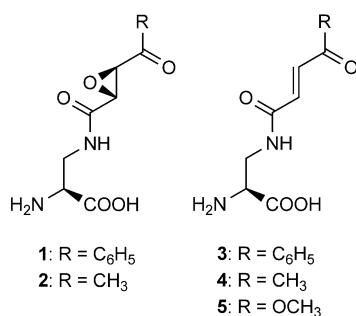


**Figure 1.** Multiple sequence alignment of GlcN-6-P synthase from *E. coli* (Ec), *C. albicans* (Ca) and *S. cerevisiae* (Sc). Identical residues are indicated by asterisks and similar residues are indicated by dots. The numbers (right-hand side) are relative to the initial Cyst residue of each sequence. Essential active centre residues identified in Ec and their counterparts in Ca and Sc are represented as white characters on black background. Residues constituting the UDP-GlcNAc binding site in Ca and their counterparts in the Sc sequence are shown within frames. Residues constituting the Q-loop and the C-loop in Ec and their counterparts in Ca and Sc are depicted with a grey background. The position of the Trp residue ("molecular gate") is indicated by an arrow.

nus, at the carboxyl side of Phe4, which facilitates identification of any products of Cys1 covalent modification in a chymotryptic digest. The properties of the enzyme, purified to near homogeneity, closely resemble those reported previously for other fungal version of this protein, including its homotetrameric structure and inhibition by UDP-GlcNAc. Although the crystal structure of the yeast enzyme is not known, there is little doubt that the constitution and 3D configuration of the active centres are very well conserved, so any conclusions drawn from the present study should be of a general character and valid for all versions of this enzyme.

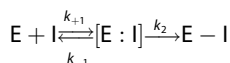
### Inactivation of GlcN-6-P synthase by L-2,3-diaminopropanoic acid derivatives

*N*<sup>3</sup>-Oxoacyl derivatives of L-2,3-diaminopropanoic acid **1–4** shown in Scheme 1 are structural analogues of the previously reported specific inhibitors of GlcN-6-P synthase (in that they contain either fumaroyl or epoxysuccinoyl fragments in the *N*<sup>3</sup>-acyl portion of the molecule) including the most efficient FMDP, **5**.<sup>[14,15]</sup>



**Scheme 1.** Structures of *N*<sup>3</sup>-oxoacyl derivatives of L-2,3-diaminopropanoic acid and FMDP.

The novel compounds **1–4** were tested as inhibitors and inactivators of yeast GlcN-6-P synthase. The inhibition assay was followed under standard conditions, with saturating concentrations of both substrates, to determine the IC<sub>50</sub> values. Enzyme inactivation was performed in the absence of L-Gln and in the presence or absence of D-Fru-6-P. Under these conditions all tested compounds inactivated the enzyme in a time- and concentration-dependent manner. The determined inactivation rate constants demonstrated a hyperbolic dependence on initial inactivator concentration, thus suggesting two-step inactivation, with formation of a reversible complex preceding covalent modification of the enzyme, according to:



where E is the free enzyme, I is an inactivator, [E:I] is the reversible complex and E-I is the inactive, covalently modified enzyme. Kinetic parameters of inactivation were determined by assuming that the relationship between  $k_{app}$  and inactivator

concentration [I] is described by Equation (1):

$$1/k_{app} = (1/k_2) + (K_{inact}/k_2) \times (1/[I]) \quad (1)$$

where  $k_2 = \ln 2/T$ ,  $K_{inact} = k_{-1}/k_1$ ,  $k_{app}$  is the apparent inactivation velocity constant at the given inhibitor concentration, and T is the minimum inactivation half-time at infinite inactivator concentration. The IC<sub>50</sub> values for inhibition and the kinetics parameters of inactivation are summarised in Table 1.

**Table 1.** Parameters of inhibition and inactivation of *S. cerevisiae* GlcN-6-P synthase by *N*<sup>3</sup>-oxoacyl derivatives of L-2,3-diaminopropanoic acid.

Compound	Inhibition		Inactivation		
	IC <sub>50</sub> [μM]	K <sub>inact</sub> [μM]	T [min]	k <sub>2</sub> [min <sup>-1</sup> ]	k <sub>2</sub> /K <sub>inact</sub> [M <sup>-1</sup> s <sup>-1</sup> ]
1	660 ± 50	450 (1250)	1.1 (1.2)	0.630 (0.578)	23.3 (7.71)
2	7350 ± 250	19400 (15200)	1.25 (1.2)	0.554 (0.578)	0.48 (0.63)
3	270 ± 30	56.5 (195)	1.3 (1.35)	0.533 (0.513)	157 (43.8)
4	5600 ± 200	15200 (8700)	1.5 (1.4)	0.462 (0.495)	0.51 (0.95)

Parameters in parentheses of inactivation determined in the presence of 10 mM Fru-6-P.

Whereas all the tested compounds demonstrated similar reactivity towards the enzyme (as reflected by the  $k_2$  and T values), they differed markedly in their affinity to the enzyme active site (as revealed by the  $K_{inact}$  values). Compounds containing the phenyl ketone terminal moiety (**1** and **3**) bound much more strongly than their counterparts containing a terminal methyl ketone (**2** and **4**). On the other hand, by analysing the effect of epoxide/double bond substitution in the **1–3** and **2–4** pairs, one can observe a slightly higher reactivity ( $k_2$ ) but lower affinity ( $K_{inact}$ ) for the epoxide compounds. Generally, compounds containing the double bond (**3** and **4**) were slightly stronger inhibitors than their respective epoxide counterparts (**1** and **2**) in terms of the IC<sub>50</sub> values. Interestingly enough, progressive yellowing of the reaction mixtures was observed during reaction of the enzyme with **1**, while no colour changes were noted in the reaction mixtures containing **2**, **3** or **4**. When inactivation of the enzyme was performed in the presence of D-Fru-6-P,  $K_{inact}$  values for **1** and **3** were substantially higher, while those for **2** and **4** were slightly lower.

### Model reactions of **1** or **3** with cysteine ethyl ester (CEE) or CGIF tetrapeptide

*S. cerevisiae* GlcN-6-P synthase, like its homologues from other sources, contains the essential N-terminal Cys residue that was previously identified as a catalytic nucleophile at the GAH active centre of the bacterial enzyme. In the yeast enzyme, Cys1 is followed consecutively by Gly, Ile and Phe residues (see Figure 1), with the carboxyl side of Phe4 being the first specific cleavage site for chymotrypsin. Therefore, CEE and the CGIF

tetrapeptide were chosen as the most appropriate low-molecular-weight substrates for the model reactions, aimed at identification of possible products.

The reaction between CEE and **1** in stoichiometric amounts was performed under pH-controlled conditions (pH 5.0, 7.0 and 8.0), under argon and at room temperature. Reaction progress was monitored by determination of the free thiol content with 5,5'-dithiobis-(2-nitrobenzoic acid) (DTNB). Consumption of CEE at pH 5.0 was very slow; on the other hand, disappearance of the CEE thiol at pH 7.0 and 8.0 was rapid: the determined second order velocity constants were 25.0 and 71.5  $\text{M}^{-1}\text{s}^{-1}$ , respectively. The reaction mixture, entirely colourless at the beginning of reaction, progressively turned yellow in a similar way as was observed for the enzyme inactivation by **1**, thus indicating formation of chromophore product(s). Samples of the reaction mixtures were collected at time intervals and analysed by reversed-phase FPLC (RP-FPLC). The results of these analyses are shown in Figure 2.

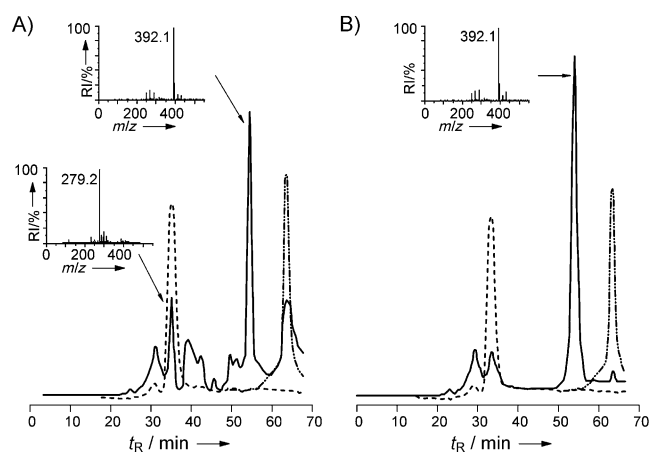


**Figure 2.** RP-FPLC analysis of components of the model 1:CEE reaction mixture. A) sample taken after 2 min; B) sample taken after 10 min. Positions of peaks corresponding to **1** (—) and CEE (---) are provided for reference. Inset: MS ESI spectra of substances indicated by the arrows. RI = relative intensity.

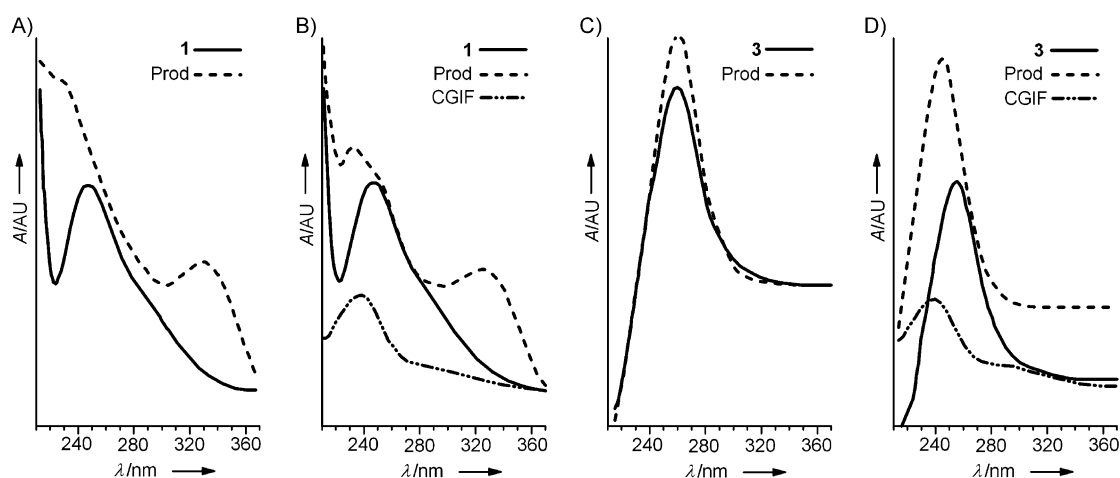
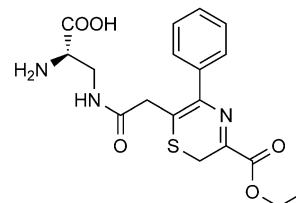


**Figure 3.** The UV/Vis spectra of substrates and products of the model reactions. A) 1:CEE; B) 1:CGIF; C) 3:CEE; D) 3:CGIF. AU = arbitrary units; Prod = product.

A progressive disappearance of peaks corresponding to substrates, and the appearance of the main product peak derived from a substance with  $(M+z)/z = 392.1$ , are evident. The product was isolated and analysed by NMR. Analysis of these data resulted in an unequivocal assignment of the structure shown in Scheme 2, from which  $M_w = 391$  can be calculated. This



**Scheme 2.** Structure of the final product of the 1:CEE model reaction, deduced from the NMR experiments.

value is in accordance with the  $M_w$  of the product giving the  $[M+H]^+ = 392.1$  signal in MS detection of the RP-FPLC analysis.

As the  $M_w$  of **1** is 278 Da and that of CEE is 149 Da,  $M_{w\text{product}}$  is 36 Da lower than the sum of  $M_{w1}$  and  $M_{w\text{CEE}}$  ( $278 + 149 = 427$ ). The UV-visible spectrum of this compound is obviously different from that of **1** (Figure 3A). The most striking difference is the presence in the product spectrum of an additional band in the 320–360 nm region, with  $\lambda_{\text{max}}$  at 330 nm.

Under the same conditions, CEE reacted rapidly with **3** at pH 7.0 and 9.0, to give a single product with  $(M+z)/z = 412.2$  (Figure 4). By assuming single protonation, the  $M_w$  of this product (411 Da) is equal to the sum of  $M_{w3}$  and  $M_{w\text{CEE}}$  (262 and 149 Da, respectively). The reaction mixture remained colourless during the entire reaction, and the overall shape of UV-visible spectrum of the isolated product was almost identical to that of **3** (Figure 3C), thus suggesting no changes in the chromophore part of the substrate upon reaction with CEE. The product was isolated and subjected to NMR analysis. The data obtained were consistent with the structure of a product of a Michael-type addition of the CEE thiol to the C5 atom of **3** (**7** in Scheme 4, below).

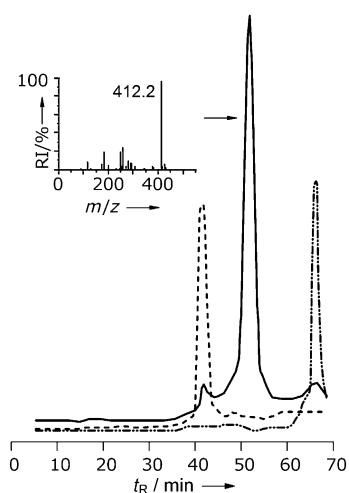


**Figure 4.** RP-FPLC analysis of components of the model 3:CEE reaction mixture. The positions of peaks corresponding to **3** (—) and CEE (---) are provided for reference. Inset: MS ESI spectrum of the product indicated by the arrow. RI = relative intensity.

The reaction of **1** with the CGIF tetrapeptide was slower than that with CEE (the second order velocity constant of the reaction at pH 7.0 was  $1.25 \text{ M}^{-1} \text{ s}^{-1}$ ), and RP-FPLC/MS analysis of the components of the reaction mixture revealed more species. In the chromatograms shown in Figure 5 one can distin-

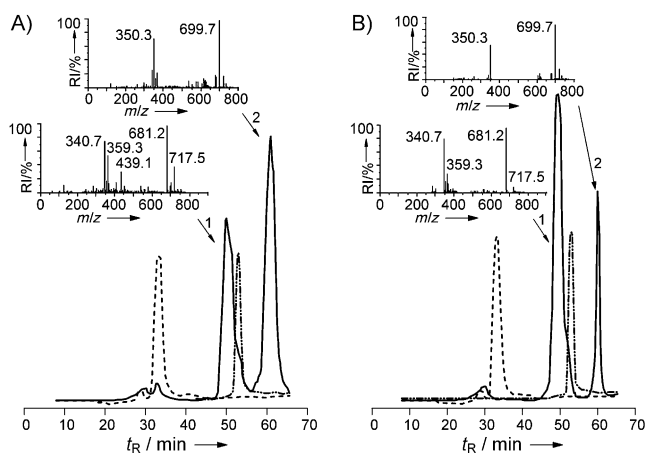


**Figure 5.** RP-FPLC analysis of components of the model 1:CGIF reaction mixture. A) sample taken after 5 min; B) sample taken after 20 min. The positions of peaks corresponding to **1** (—) and CGIF (---) are provided for reference. Inset: MS ESI spectra of substances indicated by the arrows. RI = relative intensity.

guish two additional peaks (one of them quite complex), different from those of the substrates. The intensities of these peaks changed with time, thus indicating reaction progress and conversion of intermediates into the final product. Peak 1 in chromatogram 5 A has three components. One, with  $(M+z)/z = 439.1$  and seemingly derived from CGIF ( $M_w = 438 \text{ Da}$ ), is absent from the respective peak 1 in the chromatogram shown in Figure 5 B).

Two other components of peak 1 in Figure 5 A are expected to have  $M_w$  of 716 and 680 Da, as signals of their  $[M+H]^+$  and  $[M+2H]^{2+}$  ions are present in the MS spectrum. The relative content of component 716 in the reaction mixture decreased with time, while that of component 680 increased. Peak 2, the intensity of which decreased with time, is derived from a single component with expected  $M_w = 698$  or 699 Da. One may thus conclude that signals of decreasing intensity derived from intermediates, and that these were converted eventually into the final product of 680 Da. The  $M_w$  of this product is 18 and 36 Da lower than those of the two intermediates, while the  $M_w$  of the largest putative intermediate is equal to the sum of  $M_{w1}$  and  $M_{wCGIF}$ . The UV-visible spectrum of the isolated final product (Figure 3 B) is very similar to that of the product of the reaction of **1** with CEE, thus suggesting a close similarity of chromophore regions of both compounds. This assumption was also confirmed by the progressive yellowing of the reaction mixture containing CGIF and **1**.

The overall shape of the UV-visible spectrum of the product of the reaction between **3** and CGIF was almost identical to those of the other substrates (Figure 3 D), and a single peak, different from those of the substrates and corresponding to the substance with  $(M+z)/z = 700.1$  and 351.0, was found by the RP-FPLC/MS analysis (details not shown). This finding indicates that the course of reaction between the CGIF tetrapeptide and **3**, and the chemical nature of the single product formed in this reaction are the same as for the reaction of **3** with CEE.

#### MALDI-TOF analysis of the reaction between **1** or **3** with GlcN-6-P synthase

Pure GlcN-6-P synthase was treated with **1** or **3** under conditions ensuring complete enzyme inactivation. Components of the reaction mixture were separated by electrophoresis, and protein was digested in-gel with chymotrypsin. The digests were subjected to MALDI-TOF analysis, and the obtained spectra were compared to those of the chymotryptic digest of the enzyme. Spectra of the chymotryptic digests of the native and **1**-inactivated enzymes and their difference spectrum are shown in Figure 6. The signal with the largest intensity, present only in the B) spectrum, has  $(M+z)/z = 681.2$ , identical to that of the final product of the model reaction between **1** and CGIF. On the other hand, the 439.1 signal, present exclusively in the A) spectrum, seems to be derived from the CGIF tetrapeptide.

The 439.1 signal present in the MALDI-TOF spectrum of the chymotryptic digest of native GlcN-6-P synthase was absent in the spectrum of the chymotryptic digest of the **3**-inactivated enzyme (data not shown). On the other hand, the 700.1 signal was found exclusively in the spectrum of the chymotryptic digest of the **3**-inactivated enzyme, although its intensity was low.

Both difference spectra contained the inactivated enzyme-specific signal 539.1 of unknown origin (see Figure 6).

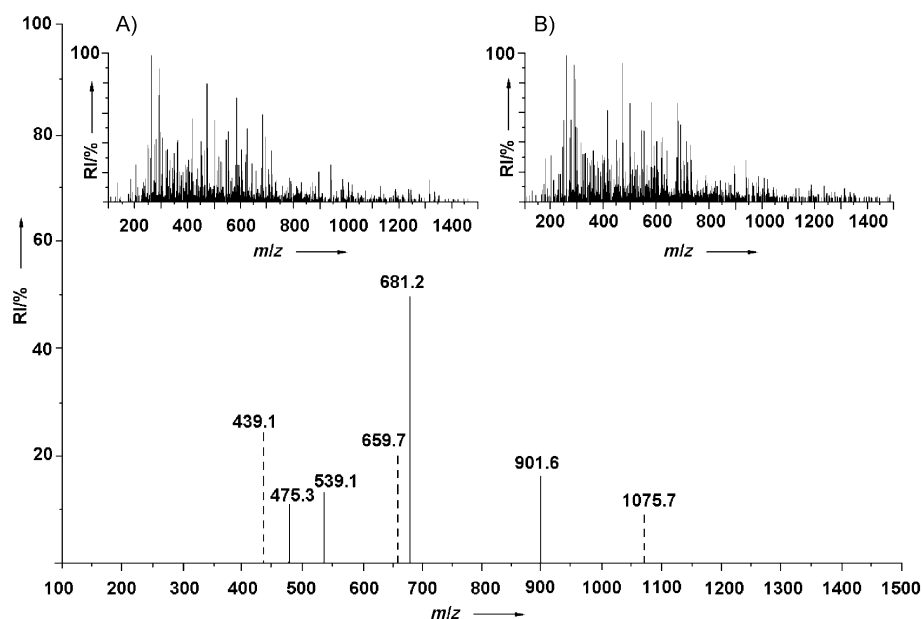


**Figure 6.** MALDI-TOF analysis of the chymotryptic digests. Difference spectrum obtained by superposition of the  $m/z$  200–800 regions of spectra A) native GlcN-6-P synthase and B) 1-modified enzyme. Peaks derived from the spectrum A) are shown as dashed lines and these from spectrum B) as solid lines. Signals present in both spectra and signals of relative intensity lower than 10% are not shown.

### Molecular modelling of inhibitor binding and its conversion by the GAH domain of GlcN-6-P synthase

The molecular modelling of **1** and **3** docked at the active site of the GAH domain of the *E. coli* GlcN-6-P synthase (PDB ID: 1GMS) has shed some light on the geometry of the complexes and on the nature of the interactions between inhibitors and amino acid residues within the active site. The conformations of the crucial amino acid residues at the active site of this template are almost identical to those in the complete “empty” enzyme (PDB ID: 1JXA),<sup>[16]</sup> including that of the “molecular gate”, Trp74, which is in the open conformation. The most important difference is the conformation of the catalytic Cys1 residue, which is locked in the inactive conformation in 1GMS while in 1JXA it is present in the active conformation. The conclusions drawn from the results of these experiments are

almost certainly valid for the purpose of studies on inhibitor binding and inactivation of yeast GlcN-6-P synthase, because all residues identified as crucial for substrate binding and catalysis in the bacterial enzyme are perfectly conserved in other versions of this enzyme, including that of *S. cerevisiae* (see Figure 1). In particular, the molecular gate in the yeast enzyme is undoubtedly the Trp87 residue.

Docking experiments revealed that both **1** and **3** bind at the active centre of GAH in a very consistent way. Clustering analysis of the resulting ligand conformations showed that only five qualitatively different solutions could be identified, and that there was only one dominant cluster of ligand conformations (containing 35 members). At the same time, the representative conformation of this cluster represented the minimum energy geometry of the complex. The second cluster contained only ten solutions, with a mean binding energy only about 0.4 kcal mol<sup>-1</sup> higher than that of the first. The differences between the particular conformations concerned only the phenyl ketone moiety of the ligand, while the positions of its diaminopropanoic skeleton and the amide bond closely resembled locations of the respective parts of the bound natural substrate, glutamine (Figure 7). The  $\alpha$ -carboxy and  $\alpha$ -amino groups of the ligands interacted with a specific set of the active-site amino acids, namely Arg73, Asp123, His86, Thr76, His77 and Gly99, in exactly the same way as the natural substrate.<sup>[17]</sup> Moreover, the amide moiety of the diaminopropanoic acid derivatives was able to form hydrogen bonds to the main chain carbonyl

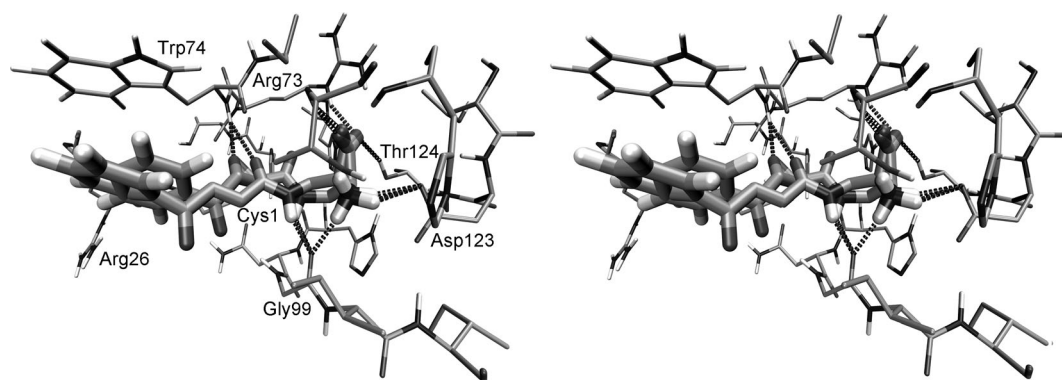


**Figure 7.** Stereoview comparison of the geometries of **1** and **3** complexed with the glutamine binding site of GlcN-6-P synthase. Interactions of ligands with Arg73, Trp74, Gly99 and Asp123 residues are indicated as black springs. Ligands are represented as thick sticks, and residues of the binding site within 4 Å of the ligands are represented as thin sticks. Trp74 is in the open conformation, and Cys1 is in the inactive conformation.

oxygen of Gly99 and the main chain amide nitrogen of Trp74. All these interactions locked the respective parts of these inhibitors very firmly inside the binding pocket. The most notable difference between the 1:GAH and BADP:GAH complexes was the presence in the former of an additional hydrogen bond acceptor (the oxirane oxygen), absent in the three molecule. As shown in Figure 7, in the 1:GAH complex, this atom participates in the interaction with the –NH– group of the Trp74 backbone. In the complex formed with **3**, the average distance between the backbone oxygen of Gly99 and the hydrogen bond donor (the –NH– nitrogen of the ligand) is 2.85 Å, while the average distance between the backbone –NH– group nitrogen of Trp74 and the amide oxygen of the ligand is 3.1 Å. The analogous distances in the 1:GAH complex, with the oxirane oxygen as the hydrogen bond acceptor, are 2.95 and 2.85 Å, respectively.

The docking experiments revealed that for inhibitors that contain the phenyl ketone moiety, that is, **1** and **3**, there is another site of specific interaction with the enzyme active centre (not present in **2** and **4**). In the bound conformation, the phenyl group of both **1** and **3** is in a position where it can participate in  $\pi$ -stacking interactions with the indole ring of Trp74. The most abundant cluster and the lowest energy conformation of the 1:GAH and 3:GAH complexes clearly show that the planes of the phenyl ring of both inhibitors and the indole ring of Trp74 face each other at an average distance of 3.5 Å, with their geometric centres located against each other. Such a relative orientation of the aromatic rings is considered optimal for  $\pi$ -stacking interactions.<sup>[18]</sup> Obviously these interactions are missing in the complexes of GAH with **2** and **4**, and this is consistent with the much lower affinity of the methyl ketone inhibitors to the enzyme, in comparison to their phenyl ketone counterparts (Table 1). Moreover, analysis of the geometries grouped in the less abundant clusters, as well as the results of preliminary molecular dynamics simulations (data not shown) suggest that the phenyl ketone moiety might also participate in favourable cation– $\pi$  interactions with the Arg26 residue, and that this might also contribute to the stronger binding of **1** and **3**, in comparison with **2** and **4**. This interaction is only possible when the Trp74 residue is in the open conformation with its indole ring pointing toward the acceptor's binding site. When the receptor used for docking has its Trp74 residue switched to the closed conformation (intersecting the ammonia channel), the most abundant conformation of the docked ligand has a completely different geometry of the phenyl ketone moiety. It points away from the binding site, thereby making any  $\pi$ – $\pi$  interactions with the Trp74 indole ring impossible. This observation explains why the stacking interactions of **1** and **3** with Trp74 must be lost when the ISOM domain of GlcN-6-P synthase is occupied by Fru-6-P, as binding of this substrate to the enzyme triggers closure of the molecular gate, due to the rotation of the indole ring by about 75°. <sup>[19]</sup> This conformational change is the most likely explanation for the substantially higher  $K_{\text{inact}}$  values determined for inactivation of GlcN-6-P synthase by **1** and **3**, in the presence of 10 mM Fru-6-P (Table 1).

The switch of the Cys1 residue to the active conformation, known to occur upon Fru-6-P binding,<sup>[20]</sup> brings its sulfhydryl group close to C6 of the **1** oxirane ring (4 Å) and brings its  $\alpha$ -amino group to a position suitable for Schiff base formation with the carbonyl group of this inhibitor. It is well known that in the catalytic mechanism of GlcN-6-P synthase, the  $\alpha$ -amino group of Cys1 participates in deprotonation of its own thiol moiety.<sup>[5,21]</sup> It seems very likely that when **1** is bound at the GAH active site instead of glutamine, the proton captured by the  $\alpha$ -amino group of Cys1 can be subsequently transferred to the oxirane oxygen, thus facilitating ring opening upon nucleophilic attack of the cysteine thiolate at C6. However, the proton might also be derived from any other active site residue, as suggested by Hollenhorst et al. in their recent studies on the mechanism of GlcN-6-P synthase inactivation by enamide and epoxyamide inhibitors.<sup>[22]</sup> The nucleophilic  $\alpha$ -amino group of Cys1 might then easily form the Schiff base with the keto group of the inhibitor, thus leading to closure of the six-membered ring. It is not clear whether there are any factors promoting the subsequent water elimination to give the final structure (corresponding to that formed in the model reaction of **1** with CEE), however, they do not seem necessary. More importantly, the substituted ring system involving  $\alpha$ -nitrogen, two carbon atoms and the sulfur of Cys1 is well accommodated at the GAH active centre, as shown in Figure 8. It seems, therefore, that formation of the final cyclic product of enzyme inactivation by **1** does not require initial binding or any major rearrangements of the participating molecules (ligand or binding site residues) except for the switch of Cys1 to the active conformation.

## Discussion

Glucosamine-6-phosphate synthase belongs to the class II subfamily of glutamine-dependent amidotransferases. Like the other members of this subfamily, the enzyme contains an N-terminal Cys1 residue that provides the reactive thiol nucleophile to participate in glutamine hydrolysis in the initial stage of GlcN-6-P-synthase-catalysed formation of glucosamine-6-phosphate. A number of reactive electrophilic glutamine analogues reacting with Cys1 of GlcN-6-P synthase (and consequently inactivating the enzyme) are known, including  $\alpha$ -diazo-ketones,  $\alpha$ -haloketones,  $\gamma$ -dimethylsulfonium salts,  $N^3$ -fumaroyl derivatives of L-2,3-diaminopropanoic acid and its epoxy derivatives.<sup>[4]</sup> So far, a detailed molecular mechanism of enzyme inactivation has been determined only for FMDP, where a Michael-type nucleophilic addition to the conjugated double bond system was, under certain conditions, followed by intramolecular cyclisation by involving the  $\alpha$ -amino group of a substituted Cys1.<sup>[10]</sup> In this paper, the results of studies on *S. cerevisiae* GlcN-6-P synthase inactivation by FMDP analogues bearing the  $N^3$ -oxoacyl functionality instead of the  $N^3$ -fumaroyl are presented. Two out of the four studied compounds contained the phenyl ketone substituents (**1** and **3**), while the remaining two had methyl ketone counterparts (**2** and **4**). The electrophilic centre was an activated double bond in **3** and **4** and an epoxide group in **1** and **2**. All four compounds inactivated yeast

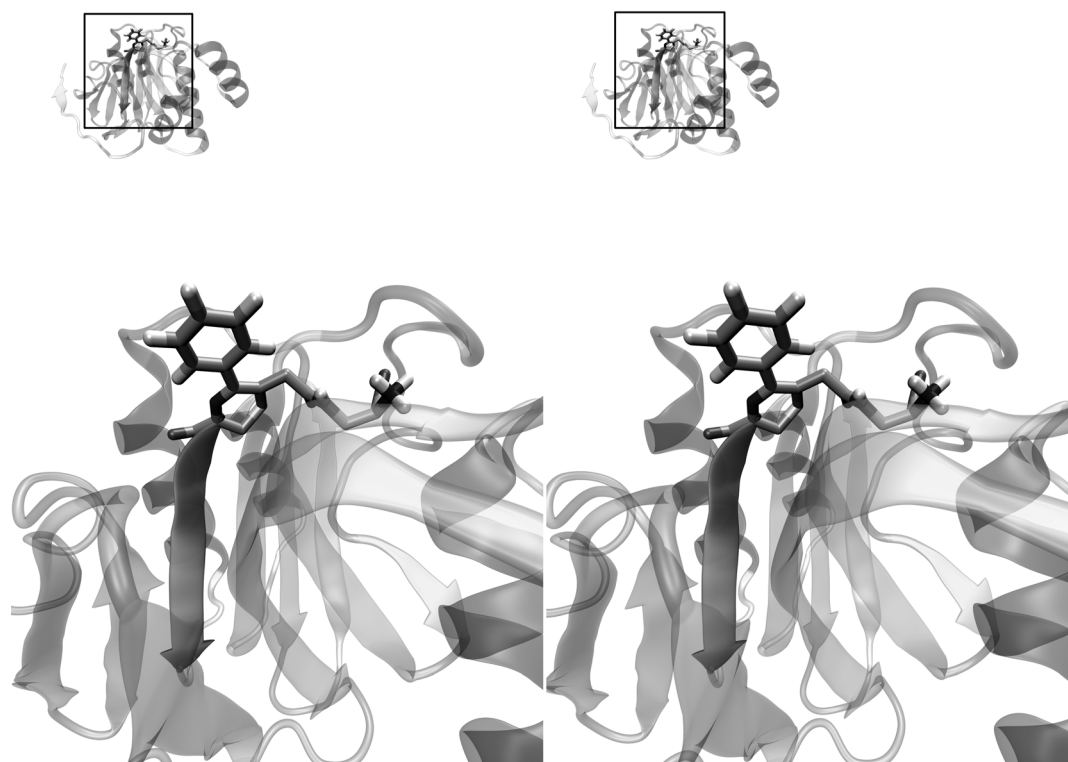
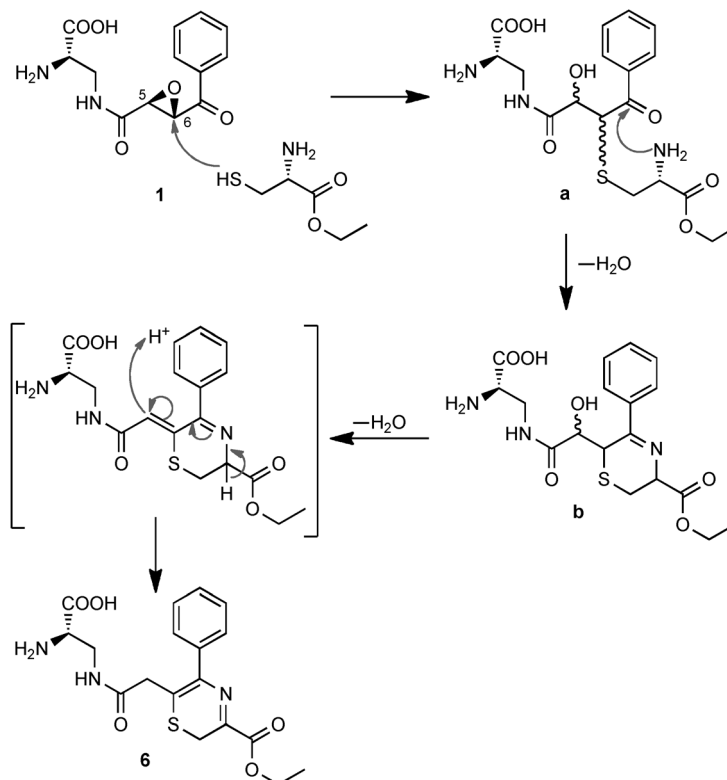


**Figure 8.** Stereoview of the geometry of the putative cyclic product of the inactivation of GlcN-6-P synthase by **1**. Top: general view at the GAH domain covalently modified by **1**. Below: binding site (enlarged). The protein is presented as a cartoon model, with the N-terminal  $\beta$ -strand in front (dark) and the Cys1 residue incorporated into the cyclic product of inactivation drawn as sticks.

GlcN-6-P synthase in time- and concentration-dependent manner. Yellowing of the reaction mixture during enzyme inactivation by **1** suggested formation of a novel chromophore system. On the other hand, substantial difference in enzyme inhibitory potential between phenyl ketone and methyl ketone compounds, and contradictory effects of Fru-6-P presence on enzyme inactivation, indicated the possibility of any undetermined specific enzyme–inhibitor interactions, triggered upon Fru-6-P binding. In order to determine the molecular mechanisms of enzyme inactivation, including the above-mentioned phenomena, we used a stepwise approach by involving studies on model reactions with low molecular-weight mimics of the enzyme catalytic residue by means of various spectroscopic techniques.

Reaction of **1** with CEE was rapid and led to the formation of a single product that was isolated and characterised by 2D NMR, MS-ESI and UV-visible spectroscopy. The structure deduced from these analyses, shown in Scheme 2, is the only one consistent with all experimental data. A possible mechanism of the reaction between **1** and CEE is presented in Scheme 3 and consists of the four main steps. Initially, the thiolane group of CEE attacks the C6 atom of **1**, to open the oxirane ring and form the S–C bond, and thus gives the putative intermediate (**a**). In the second step, the  $\alpha$ -amino group of CEE at-



**Scheme 3.** Hypothetical mechanism of reaction between **1** and CEE.

tacks C7 of the ketone carbonyl to form a Schiff base and closes the six-membered ring. A water molecule is eliminated during this condensation, and the putative intermediate (**b**) is formed. Subsequently, elimination of another water molecule (a reaction that is characteristic for  $\beta$ -hydroxy acids and its derivatives and noted also in some biological systems without participation of any enzymatic catalysis)<sup>[23]</sup> gives rise to the C5=C6 double bond. This reaction seems to be favoured by the presence of electron-withdrawing substituents at C6 that should enhance acidity of the proton there and thus stimulate its removal as the first step of  $\beta$ -elimination. Formation of a conjugated double system is another factor stimulating this reaction step. Finally, the conjugated  $\pi$  electron system is isomerised to the (probably more stable) intra-ring system in **6** that is the final product of reaction between **1** and CEE, as identified by NMR.

Obviously, in **1** there are two possible electrophilic sites for nucleophilic attack: the C5 and C6 carbons. Preference for C6 over C5 results from at least two factors: 1) a quite significant difference in the electrostatic potential (ESP),  $-0.229$  at C5 and  $+0.090$  at C6, thus favouring attack at the latter; 2) if the C–S bond was formed with C5, a seven-membered ring would be formed at the second stage. Such a system is much less stable than a six-membered ring and thus unlikely to be formed. Therefore it seems that, in this case, subsequent formation of the stable ring system is an important factor stimulating direction of the initial nucleophilic attack. However, it is worth mentioning that there are numerous examples of epoxide-containing inhibitors of other cysteinyl enzymes, including E-64 (a well-known inhibitor of cysteinyl proteases), that demonstrate significant regiospecific preference of the nucleophilic attack; this was also evident in model reactions with low molecular-weight thiols.<sup>[24]</sup>

Intermediates corresponding to (**a**) and (**b**) in Scheme 3 were identified in the reaction mixture of CGIF and **1**. This reaction was much slower, and thus allowed capturing of intermediates and obtaining their MS-ESI spectra. Although we were not able to isolate the pure final product of this reaction and determine its structure by NMR, the  $M_w$  determined by MS-ESI corresponding to  $(M_{w1} + M_{wCGIF}) - (2 \times 18)$ , and the fact that the UV-visible spectrum of this compound and that of the product of reaction between **1** and CEE are apparently identical seem to provide strong evidence that the substituted ring systems formed in both reactions are identical.

Results of MALDI-TOF analysis of components of the chymotryptic digests obtained upon treatment of native and **1**-inactivated GlcN-6-P synthase, especially the 681.2 signal substituting the 439.1 signal, clearly suggest that reaction of **1** with the enzyme leads to the formation of the same derivative of the CGIF tetrapeptide that was detected in the model reaction **1**:CGIF. The possibility of formation of a thiazine ring is further supported by the identical colour changes noted in both reaction mixtures. Further support arises from the results of the molecular modelling shown in Figure 8, which confirm the possibility of accommodation of the ring system at the active site of the GAH domain. On the other hand, docking of **1** at the active site of GAH revealed the possibility of attack by

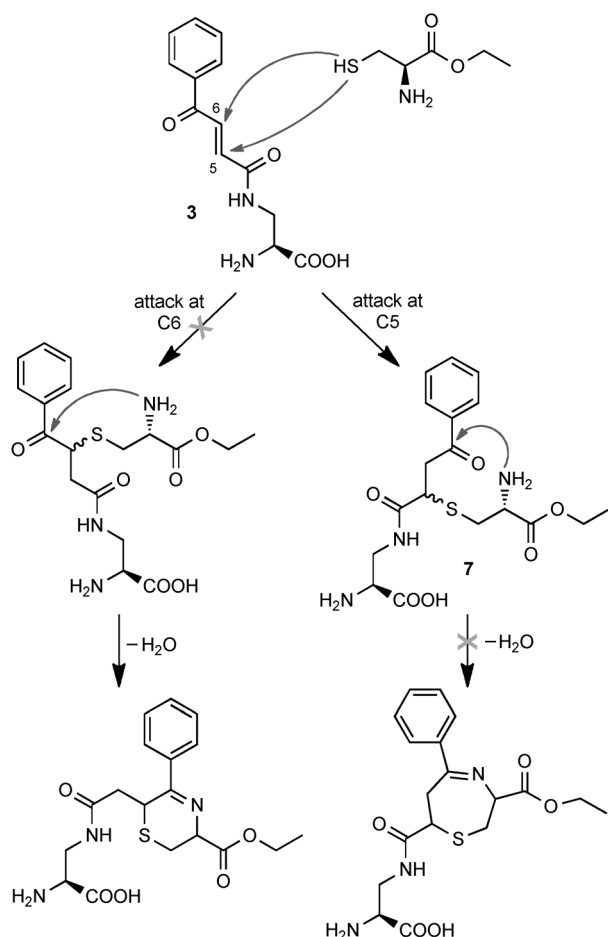
Cys1 thiol at C6 of the inhibitor molecule, which is a prerequisite for the subsequent formation of the thiazine ring system. This attack should be additionally facilitated by the preceding protonation of the epoxide oxygen. The proton might be derived from a water molecule, with participation of the N-terminal  $\alpha$ -amino group of Cys1, thus serving as a general base catalyst, as has been similarly proposed to take place during L-Gln hydrolysis when catalysed by GlcN-6-P synthase.<sup>[21]</sup> Such facilitated protonation and stabilisation of the final product (and probably also the intermediates) by the hydrogen bond network seem to be the reason for the faster reaction of GlcN-6-P synthase with **1**, in comparison to the model reaction of CGIF with this compound.

The mechanism of reactions of **3** with CEE, CGIF and GlcN-6-P synthase seems to be much different from that of its epoxide analogue **1**. For **3**, there is little doubt that all three reactions stopped after the initial Michael-type addition of the cysteinyl thiol nucleophile to the conjugated enone system. This is clearly suggested by the results of RP-FPLC/MS (model reactions: single products,  $M_w$  of the products equal to the sum of substrate  $M_w$ s; enzyme inactivation: the 700.1 signal substituting the 439.1 signal in MALDI-TOF spectrum of chymotryptic digests) and UV-visible analysis (shape of the product spectrum similar to those of the substrates, no yellowing of the reaction mixture). However, the target of the initial nucleophilic attack (C5 or C6) is not clear, but in our opinion (and consistently with the <sup>1</sup>H NMR data) this should be the C5 atom. Both atoms bear negative EPS values ( $-0.244$  at C5 and  $-0.155$  at C6), so there is no clear electrostatic preference. On the other hand, if assuming attack of the thiol group of CEE, CGIF and Cys1 of the enzyme on C6, subsequent formation of the six-membered ring (Scheme 4) would seem unavoidable, while the formation of a Schiff base (theoretically possible after attack at C5), would result in an unstable seven-membered ring. However, the possibility of formation of any cyclic products was excluded by the results of spectroscopic analyses.

Therefore attack at C6 and subsequent formation of a stable six-membered ring is unlikely to occur. One may thus conclude that attack at C5 results in formation of **7** as the final product, without any further conversion/rearrangement. Notably, the same direction of the initial nucleophilic attack was previously found in reactions of FMDP **5** with L-cysteine or with *E. coli* GlcN-6-P synthase.<sup>[10]</sup>

One of the most surprising findings was the unfavourable effect of Fru-6-P on GlcN-6-P inactivation by **1** and **3**, as all previous reports suggested that binding of this substrate to GlcN-6-P synthase facilitates enzyme inactivation by reactive glutamine analogues. This effect, originally found with inactivation of the *E. coli* GlcN-6-P synthase by **5**<sup>[25]</sup> was later explained as a consequence of the ordering of the GAH active centre upon Fru-6-P binding at ISOM.<sup>[19]</sup> This explanation seems valid for inactivation of the *S. cerevisiae* enzyme by **2** and **4**, but in the case of the reaction involving **1** and **3** it is apparently prevented due to interactions between the aromatic ring of the inhibitors and the indole ring of Trp87.

The mechanism of GlcN-6-P synthase inactivation by **1** and **3** is clearly different from that found previously by Kucharczyk



**Scheme 4.** Alternative mechanism of reaction between **1** and CEE.

et al. for **5** with the bacterial enzyme.<sup>[25]</sup> The only similarity is the fact that both mechanisms are valid for model systems (L-cysteine or its ester, N-terminal oligopeptide) and for the whole enzyme. Probably, this is because Cys1 is the only catalytic residue at the active centre of GAH, and therefore the whole enzyme might react with glutamine analogues like the large,  $\alpha$ -carboxyl substituted cysteine derivative. All the other aspects of these mechanisms (sequence of the steps, structure of the intermediates, final products) are different and seem to be specific for particular types of inactivator structure. In the reaction involving **5**, the presence of a methyl ester group is crucial for the first-step cyclisation, thus leading to the formation of the substituted succinimide intermediate, promoted under denaturing conditions.<sup>[26]</sup> However, the initial cyclisation depicted in Scheme 1 is possible because of the properly positioned keto functionality in **1**, thereby giving rise to the Schiff base formation. Therefore, the reaction of **1** with GlcN-6-P synthase represents an entirely novel mechanism of enzyme inactivation by a glutamine analogue, with the formation of an exceptional, specific, chromophoric ring system as the final product.

## Conclusions

$N^3$ -Oxoacyl derivatives of L-2,3-diaminopropanoic acid react with CEE, CGIF tetrapeptide and GlcN-6-P synthase. Interactions of the phenyl rings present in some of these compounds with the indole ring of the tryptophan residue, which constitutes the "molecular gate" at the enzyme active centre, strongly influence inhibitor binding. The bound inhibitors react with the N-terminal catalytic Cys1 residue in the same way as the low-molecular-weight mimics of the enzyme N terminus (i.e., CEE and CGIF). Formation of the C–S bond upon attack of the cysteine thiolane at the electrophilic centre of an inhibitor (epoxide or conjugated carbon–carbon double bond) is the first step of these reactions. The presence of an appropriately positioned keto functionality in the compounds studied affords an opportunity for subsequent cyclisation, as a result of the Schiff base formation upon reaction with the  $\alpha$ -amino group of a cysteinyl substrate. Substantial differences in the target of the initial nucleophilic attack and further rearrangements of an intermediate were found for the structurally related compounds, **1** and **3**. Attack at C6, followed by formation of the substituted 1,4-thiazine-3-en derivative are elements of reactions involving compound **1**, which contains an epoxide functionality. On the other hand, **3**, which contains a conjugated double bond, is attacked at C5, and the product of a simple Michael-type addition does not appear to undergo any further rearrangement.

## Experimental Section

**Chemicals:** L-2,3-diaminopropanoic acid derivatives **1–4** were synthesised as described previously.<sup>[11]</sup> The CGIF tetrapeptide was synthesised manually by a solid-phase peptide synthesis method by using the Fmoc/But strategy. Other chemicals, including CEE, were from Sigma.

**Plasmids, yeast and bacterial strains and culture conditions:** *S. cerevisiae* BJ1991 (*MAT $\alpha$* , *pep4–3*, *prb1*, *ura3*, *leu2*, *trp1*) was provided by I. Purvis (Glaxo Group Research, Greenwood, UK). *E. coli* DH5 $\alpha$ F9 (Life Technologies, Carlsbad, CA) was used for plasmid selection and amplification. The YEpGW42 plasmid (8.7 kb), carrying the *S. cerevisiae* *GFA1* gene on a 3.5 kb EcoRI fragment inserted into Yep352,<sup>[26]</sup> was a gift from W. Tanner (Regensburg, Germany). YEpMA91 was a yeast shuttle vector carrying the *LEU2* marker and the promoter and terminator from *PGK1* separated by a BglII site.<sup>[27]</sup> The YRS-23–3 strain overproducing GlcN-6-P synthase was obtained by transformation of *S. cerevisiae* BJ 1991 cells with the YEpRS23–3 plasmid, containing the *GFA1* gene under control of the *PGK1* promoter, and based on the YEpMA91 vector. Detailed protocols for plasmid construction and yeast transformation are those described previously for the preparation of *S. cerevisiae* cells overproducing *C. albicans* GlcN-6-P synthase.<sup>[13]</sup> Yeast cells were grown in YPD medium (2% glucose, 2% Bactopeptone, 1% yeast extract).

### Purification of the enzyme

*I. Preparation of crude extract.* YRS-23–3 cells (10 g wet weight) from an overnight culture in YPD were harvested by centrifugation (5000 g, 10 min) and washed with buffer A (potassium phosphate (20 mM, pH 7), EDTA (1 mM)). Cells were mixed (1:1 v/v) with buffer B (potassium phosphate (20 mM, pH 7), EDTA (1 mM), dithio-

threitol (DTT, 1 mM)) and then disrupted by using a French press. Cell debris was spun down (15000g, 20 min), and the supernatant was saved as a crude extract.

**II. Protamine treatment.** A solution containing 1% protamine sulfate in buffer B was added dropwise to the crude extract (1 mL per 140 mg of protein present in the crude extract) and stirred moderately. The precipitated solid was removed by centrifugation (15000g, 20 min) and the supernatant was saved.

**III. Ammonium sulfate precipitation.** Ammonium sulfate solution in buffer B (80% saturation) was added dropwise to the protamine sulfate supernatant, and stirred gently until 55% saturation with respect to ammonium sulfate was reached. The obtained suspension was centrifuged (15000g, 20 min), the supernatant was discarded and precipitate was dissolved in buffer B (10 mL).

**IV. Polyethylene glycol precipitation.** A solution containing 50% polyethylene glycol ( $M_w$  6000–7500, 2.5 mL) was added dropwise to the gently stirred solution from the previous step. The obtained suspension was centrifuged (15000g, 20 min), the supernatant was discarded and the precipitate was dissolved in a minimal amount of buffer C (composition as for B, supplemented by Fru-6-P (1 mM)).

**V. Ion-exchange chromatography.** A solution from the previous step was loaded onto a Resource Q FPLC column equilibrated with buffer D (Tris-HCl (25 mM, pH 7.5), EDTA (1 mM), DTT (1 mM), Fru-6-P (1 mM)). The column was washed with buffer D (5 mL) and elution was performed with a linear KCl gradient (0–0.5 M) in buffer D at 1.0 mL min<sup>-1</sup>. Active fractions were pooled and concentrated by ultrafiltration with a Centricon 10 device.

**VI. Size-exclusion chromatography.** The pooled concentrated active fraction from the previous step was loaded on a Superdex 200 HR 10/30 column equilibrated with buffer D containing NaCl (0.15 M). Protein was eluted with the same buffer (0.5 mL min<sup>-1</sup>). Active fractions were pooled. Steps I–IV were run at 4 °C, and steps V and VI were run at room temperature.

**Determination of GlcN-6-P synthase activity:** A standard incubation mixture consisted of Fru-6-P (10 mM), L-glutamine (10 mM), EDTA (1 mM), DTT (1 mM) and potassium phosphate (50 mM, pH 7.0), with appropriately diluted enzyme preparation and inhibitors where necessary. Final concentration of the pure GlcN-6-P synthase was 0.5–1.0 μg mL<sup>-1</sup>. The reaction was started by adding the enzyme, then incubated at 37 °C for 30 min and terminated by boiling for 1 min. The concentration of GlcN-6-P produced by the enzyme was determined by a modified Elson-Morgan procedure,<sup>[28]</sup> and this increased linearly for at least 60 min. One unit of specific activity was defined as an amount of enzyme that catalysed the formation of 1 μmol GlcN-6-P min<sup>-1</sup> mg protein<sup>-1</sup>.

**Molecular weight determination:** Gel filtration was performed on a Superdex 200 HR 10/30, and eluted at 0.5 mL min<sup>-1</sup> with potassium phosphate (25 mM, pH 6.8) containing NaCl (0.15 M), DTT (1 mM) and EDTA (1 mM). Protein elution was followed at 280 nm, and GlcN-6-P synthase activity was measured colorimetrically in 0.5 mL samples. Discontinuous SDS-PAGE was performed by the method of Laemmli,<sup>[29]</sup> with a 5% stacking gel and a 7.5% separating gel.

**Determination of an isoelectric point:** Chromatofocusing was performed on a Mono P HR 5/5 column. The purified GlcN-6-P synthase (2 μg) was dissolved in Bis-Tris-HCl, (25 mM, pH 6.3) as a starting buffer, and a pH 6–4 gradient was generated during the elution with Polybuffer 74 solution (20 mL, diluted 1:10 in water, pH 4).

Samples (0.5 mL) were collected, and pH and GlcN-6-P synthase activity were measured.

**Determination of kinetics of inactivation of GlcN-6-P synthase by glutamine analogues:** Incubation mixtures containing of GlcN-6-P synthase (5 μg), potassium phosphate (50 mM, pH 7.0), EDTA (1 mM), inactivators at various concentrations and Fru-6-P (10 mM) if necessary, in a total volume of 1 mL were incubated at 25 °C. To follow the inactivation of the enzyme, aliquots (200 μL) were withdrawn from the mixtures, applied to the tops of mini-columns packed with gel slurry (1 mL; Sephadex G-25 equilibrated with potassium buffer (50 mM, pH 7.0)) and centrifuged (500g, 1 min, 4 °C). Under these conditions the unbound inhibitor was separated from the enzyme, and protein was recovered in clean test tubes. Appropriate eluent aliquots were used for the determination of the residual enzyme activity.

**Reaction of CEE with glutamine analogues or CGIF tetrapeptide:** Equimolar amounts of CEE or CGIF tetrapeptide with **1** or **3** (1 mmol each) were dissolved in oxygen-free potassium phosphate buffer (10 mL, 5 mM, pH 5.0, 7.0 or 8.0), and the mixtures were kept at 25 °C under argon. Samples of the reaction mixture (0.2 mL) were collected at various time intervals. Aliquots (50 μL) were taken for immediate determination of free thiol content, and components present in the remaining aliquots (150 μL) were separated by RP-FPLC on an RPC column. Elution was with methanol/water, and detection was at 212 nm. Fractions containing components were pooled, evaporated to remove methanol, frozen and lyophilised. Final products of reactions between CEE and compounds **1** and **3**, (i.e., **6** and **7**, respectively) were isolated and analysed by NMR. The NMR spectra of product **6** from HMBC and HSQC experiments are provided in the Supporting Information. Data for product **7**: <sup>1</sup>H NMR (300 MHz, D<sub>2</sub>O): δ = 7.68–7.45 (m, 5H; Ph), 4.29 (q, *J* = 4.8 Hz, 2H; CH<sub>2</sub>CH<sub>2</sub>O), 4.16 (t, *J* = 11.1 Hz, 1H; NHC(O)CHSCH<sub>2</sub>), 3.98 (t, *J* = 5.5 Hz 1H; SCH<sub>2</sub>(NH<sub>2</sub>)CHCOOEt), 3.91 (t, *J* = 8.3 Hz, 1H; HOOC(NH<sub>2</sub>)CHCH<sub>2</sub>NH), 3.65–3.54 (dd, *J* = 6.5 Hz, 2H; HOOC(NH<sub>2</sub>)CHCH<sub>2</sub>NH), 3.28 (d, *J* = 6.7 Hz, 2H; SCHCH<sub>2</sub>(O)Ph), 3.18–3.11 (dd, *J* = 12.3 Hz, 2H; SCH<sub>2</sub>CH(NH<sub>2</sub>)COOEt), 1.18 (t, *J* = 6.6 Hz, 3H; CH<sub>3</sub>CH<sub>2</sub>O).

**Determination of free thiol content:** Aliquots (50 μL) were collected from the reaction mixtures and combined with potassium phosphate (900 μL, pH 7.0) and DTNB (50 μL, 3 mM). Mixtures were kept for 5 min at room temperature, and then the absorption at 412 nm was measured.

**Inactivation of GlcN-6-P synthase and preparation of chymotryptic/tryptic digests:** Homogenous GlcN-6-P synthase (2 mg, ~6 nmol) dissolved in potassium phosphate buffer (20 mM, pH 7.0, 4 mL) was incubated at 25 °C under argon with **1** or **3** (1 mM) or alone. Samples (20 μL) were collected and subjected to SDS-PAGE electrophoresis. Native or inactivated protein present in the sample were digested by sequencing-grade chymotrypsin or by trypsin by using the in-gel proteolysis procedure of Shevchenko et al.<sup>[30]</sup>

**Molecular modelling:** The structure of the receptor for docking calculations was built on the basis of the PDB file 1GMS (complex of the GAH domain of *E. coli* glucosamine-6-phosphate synthase with γ-glutamyl hydroxamate).<sup>[17]</sup> As the X-ray-derived protein structure lacks all hydrogens, the hydrogen atoms bound to aromatic fragments and heteroatoms were added for the simulations with the pdb2gmx tool included in the GROMACS package (<http://www.gromacs.org>), and the complete structure was energy minimised by using the gromos 43a2 forcefield.<sup>[31]</sup> The resulting “minimised structure” was then used for the subsequent flexible

docking simulations with the AutoDock 4.2 suite of programs.<sup>[32]</sup> AutoDock atom types and Gasteiger partial charges were assigned to all atoms by means of the accompanying AutoDockTools Python script `prepare_receptor4`. The grid box (60×60×60 grid-points), embracing the entire binding site, was calculated by the `autogrid4` tool with default spacing of 0.375 Å. The structures of ligands **1** and **3**, as well as the structure of the putative cyclic product of enzyme covalent inactivation, were built by using the InsightII molecular modelling environment from Accelrys.<sup>[33]</sup> The ligands were prepared for docking simulations by AutoDockTools script `prepare_ligand4`. Ligand atom types were determined at this stage; Gasteiger partial charges were calculated and assigned to all atoms, and suitable single bonds were marked as flexible. The Lamarckian genetic algorithm (LGA) was used as the search protocol. The actual docking simulations were carried out with 50 independent runs and initial populations of 150 solutions. A maximum of 25 million energy function evaluations and 27 000 generations were set to achieve convergence and avoid premature search-procedure termination. The rates of crossover and mutations were set to 0.8 and 0.02, respectively. After the final docking, the resulting ligand conformations were grouped with an RMSD clustering tolerance of 1.8 Å for analysis. Atomic charge distribution in ligands was calculated by means of the GAMESS package<sup>[34]</sup> at an HF/6-31G\*\* level to obtain the ESP charges.

**Other methods:** Protein concentration was assayed by the Bradford procedure<sup>[35]</sup> with bovine serum albumin as a standard. The MS ESI spectra of substrates and products of the model reactions were taken with the Agilent 1100 LC MS system equipped with the quadrupole detector. MALDI-TOF of the peptide mixtures present in chymotryptic/tryptic digests was performed in an Applied Biosystem Voyager-DE STR. NMR spectra were taken by using Varianplus 300 MHz and 500 MHz instruments.

## Acknowledgements

Financial support of these studies by the Polish Ministry for Science and Higher Education is gratefully acknowledged.

**Keywords:** enzyme inhibitors • epoxides • molecular modeling • reaction mechanisms

- [1] F. Massière, M.-A. Badet-Denisot, *Cell. Mol. Life Sci.* **1998**, *54*, 205–222.
- [2] E. Borowski, *Il Farmaco* **2000**, *55*, 206–208.
- [3] K.-C. Chou, *J. Proteome Res.* **2004**, *3*, 1284–1288.
- [4] For reviews, see: a) S. Milewski, *Biochim. Biophys. Acta Protein Struct. Mol. Enzymol.* **2002**, *1597*, 173–192; b) P. Durand, B. Golinelli-Pimpaneau, S. Mouilleron, B. Badet, M.-A. Badet-Denisot, *Arch. Biochem. Biophys.* **2008**, *474*, 302–317.
- [5] S. Mouilleron, M.-A. Badet-Denisot, B. Badet, B. Golinelli-Pimpaneau, *Arch. Biochem. Biophys.* **2011**, *505*, 1–12.
- [6] J. Raczynska, J. Olchoway, P. V. Konariev, D. I. Svergun, S. Milewski, W. Rypniewski, *J. Mol. Biol.* **2007**, *372*, 672–678.
- [7] Y. Nakaishi, M. Bando, H. Shimizu, K. Watanabe, F. Goto, H. Tsuge, K. Kondo, M. Komatsu, *FEBS Lett.* **2009**, *583*, 163–167.
- [8] N. Floquet, C. Richez, P. Durand, B. Maigret, B. Badet, M.-A. Badet-Denisot, *Bioorg. Med. Chem. Lett.* **2007**, *17*, 1966–1970.
- [9] S. Milewski, H. Chmara, R. Andruszkiewicz, E. Borowski, *Biochim. Biophys. Acta Protein Struct. Mol. Enzymol.* **1985**, *828*, 247–254.
- [10] N. Kucharczyk, M.-A. Denisot, F. Le Goffic, B. Badet, *Biochemistry* **1990**, *29*, 3668–3676.
- [11] R. Andruszkiewicz, R. Jędrzejczak, T. Zieniawa, M. Wojciechowski, E. Borowski, *J. Enzyme Inhib.* **2000**, *15*, 429–441.
- [12] B. Badet, P. Vermoote, P. Y. Haumont, F. Lederer, F. Le Goffic, *Biochemistry* **1987**, *26*, 1940–1948.
- [13] S. Milewski, D. Kuszczak, R. Jędrzejczak, R. J. Smith, A. J. P. Brown, G. Gooday, *J. Biol. Chem.* **1999**, *274*, 4000–4008.
- [14] R. Andruszkiewicz, H. Chmara, S. Milewski, E. Borowski, *Int. J. Peptide Protein Res.* **1986**, *27*, 449–453.
- [15] R. Andruszkiewicz, S. Milewski, E. Borowski, *J. Enzyme Inhib.* **1995**, *9*, 123–133.
- [16] A. Teplyakov, G. Obmolova, B. Badet, M.-A. Badet-Denisot, *J. Mol. Biol.* **2001**, *313*, 1093–1102.
- [17] M. N. Isupov, G. Obmolova, S. Butterworth, M.-A. Badet-Denisot, B. Badet, I. Polikarpov, J. A. Littlechild, A. Teplyakov, *Structure* **1996**, *4*, 801–810.
- [18] E. C. Lee, D. Kim, P. Jurečka, P. Parakeshwar, P. Hobza, K. S. Kim, *J. Phys. Chem. A* **2007**, *111*, 3446–3457.
- [19] S. Mouilleron, M.-A. Badet-Denisot, B. Golinelli-Pimpaneau, *J. Biol. Chem.* **2006**, *281*, 4404–4412.
- [20] S. Mouilleron, M.-A. Badet-Denisot, B. Golinelli-Pimpaneau, *J. Mol. Biol.* **2008**, *377*, 1174–1185.
- [21] A. Teplyakov, C. Leriche, G. Obmolova, B. Badet, M.-A. Badet-Denisot, *Nat. Prod. Rep.* **2002**, *19*, 60–69.
- [22] M. A. Hollenhorst, I. Ntai, B. Badet, N. L. Kelleher, C. T. Walsh, *Biochemistry* **2011**, *50*, 3859–3861.
- [23] C. Machacek-Pitsch, P. Rauschenbach, H. Simon, *Biol. Chem. Hoppe-Seyler* **1985**, *366*, 1057–1062.
- [24] Y. Yabe, D. Guillaume, D. H. Rich, *J. Am. Chem. Soc.* **1988**, *110*, 4043–4044.
- [25] B. Badet, P. Vermoote, F. Le Goffic, *Biochemistry* **1988**, *27*, 2282–2287.
- [26] G. Watzele, W. Tanner, *J. Biol. Chem.* **1989**, *264*, 8753–8758.
- [27] S. M. Kingsman, D. Cousens, C. A. Stanway, A. Chambers, M. Wilson, A. J. Kingsman, *Methods Enzymol.* **1990**, *185*, 329–341.
- [28] M. Kenig, E. Vandamme, E. P. Abraham, *J. Gen. Microbiol.* **1976**, *94*, 46–54.
- [29] U. K. Laemmli, *Nature* **1970**, *227*, 680–685.
- [30] A. Shevchenko, M. Wilm, O. Vorm, M. Mann, *Anal. Chem.* **1996**, *68*, 850–858.
- [31] a) B. Hess, C. Kutzner, D. van der Spoel, E. Lindahl, *J. Chem. Theory Comput.* **2008**, *4*, 435–447; b) H. J. C. Berendsen, D. van der Spoel, R. van Drunen, *Comput. Physics Commun.* **1995**, *91*, 43–56.
- [32] G. M. Morris, R. Huey, W. Lindstrom, M. F. Sanner, R. K. Belew, D. S. Goodsell, A. J. Olson, *J. Comput. Chem.* **2009**, *30*, 2785–2791.
- [33] *Insight II*; Accelrys Inc., San Diego, CA.
- [34] M. W. Schmidt, K. K. Baldridge, J. A. Boatz, S. T. Elbert, M. S. Gordon, J. H. Jensen, S. Koseki, N. Matsunaga, K. A. Nguyen, S. Su, T. L. Windus, M. Dupuis, J. A. Montgomery, Jr., *J. Comput. Chem.* **1993**, *14*, 1347–1363.
- [35] M. M. Bradford, *Anal. Biochem.* **1976**, *72*, 248–254.

Received: September 15, 2011

Published online on November 28, 2011